

Application of response surface methodology for the photo degradation of dye using ZnO nanorods loaded on the activated carbon

Hossein Kazemi, Maryam Rajabi*, Bahareh Fahimirad

Department of Chemistry, Semnan University, Semnan, Iran

Article history:

Received: 05/ May /2018

Received in revised form: 23/Oct/2018

Accepted: 15/Nov/2018

Abstract

In this work, ZnO with a nanorod morphology loaded on activated carbon (ZnO NRs-AC) was synthesized using the co-precipitation method for the photo-degradation of malachite green (MG) under the UV light. The photo-catalyst was characterized using various analytical techniques including XRD and FE-SEM. The Box-Behnken design (BBD) combined with the response surface methodology (RSM) was applied for the optimization of the influential parameters. The optimum values for the parameters involved were as follow: photo-catalyst dosage, 16 mg; MG concentration, 30 mg L⁻¹; and reaction time was 46 min. Studying the effect of foreign ions on the performance of the photo-catalytic process indicated the stability of ZnO NRs-AC in the photo-catalytic degradation of MG. According to the Langmuir–Hinshelwood (L–H) kinetic model, the kinetic degradation of MG followed a pseudo-first order kinetic model.

Keywords: ZnO nanorods, Activated carbon, Malachite green, UV light, Box-Behnken design, Kinetic model.

1. Introduction

Many industries use different dyes to paint their products and procreate a wide volume of these dyes in the resulting wastewater. Due to the toxicity of these dyes, the presence of low amounts of the min wastewater is highly undesirable. Thus the discharge of this polluted wastewater can pose severe environmental threats and human health risks [1]. Malachite green (MG) is a cationic triphenyl methane dye (Table 1) used in the textile industry for dyeing leather, silk, cotton, and wool. MG is a hazardous compound, having a variety of toxic effects on mammalian cells and causing

reproductive problems in rabbits, fish, etc.[2]. Several methods such as coagulation and flocculation [3], biological treatment [4], photo-catalytic processes [5], advanced oxidation processes [6], and adsorption [7] are good choices for wastewater treatment for removal and degradation of dyes. The photo-catalytic oxidation processes based on semi-conductors as the photo-catalysts are used as the promising techniques in ecosystem protection. These processes are based on the generation of powerful oxidizing radicals, especially hydroxyl radicals, for the degradation of the organic pollutants present in wastewaters [8-

*.Corresponding author: Associate Professor of Analytical Chemistry, Faculty of Chemistry, Semnan University, Semnan, Iran. E-mail: mrjajabi@semnan.ac.ir

11]. The mechanism of photo-catalytic oxidation for the degradation of dyes involves many steps. In this process, the catalyst surface is excited by irradiated UV or visible light and electron-hole pairs are generated. The holes can oxidize water molecules or hydroxide ions to produce hydroxyl radicals, which oxidize dyes and organic pollutants strongly and non-selectively [12]. The metal oxides such as TiO₂ [13], ZnO [14], Cu₂O [15], WO₃ [16], V₂O₅ [17], and CeO₂ [18] have been synthesized and investigated for the photodegradation of pollutants. Among the various semi-conductors employed, ZnO is known to be a good photo-catalyst for the degradation of several environmental contaminants due to its high photosensitivity [19]. Zinc oxide (ZnO) can be obtained with different morphologies. Types of morphologies of ZnO is such as: Nanorods, tubes, belts, flower, wires and etc. Preparation of zinc oxide is performed in a variety of ways, including: thermal evaporation [20], chemical vapor deposition [21], electro-deposition [22] and hydrothermal methods [23,24]. Therefore, some recent efforts have focused on the preparation of ZnO nanostructure material with different morphologies.

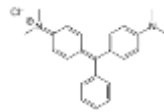
The properties of ZnO such as sizes, shapes, and dimensions show great impact on the catalytic performances. Furthermore, ZnO with various morphologies can have a significant effect on the degradation efficiency of the photocatalytic process.

Meanwhile, ZnO nanorods show a high photocatalytic activity [25].

For a better efficiency of the photodegradation processes, an adsorbent with a high pollutant adsorption capability such as activated carbon (AC) is also added as a support for ZnO. AC is a form of carbon that has a large surface area to adsorb pollutants. Modification of ZnO with AC can be an efficient way to reduce recombination of charge carriers and improve the photo-catalytic activity [26].

In this work, ZnO with a nanorod morphology supported on AC (ZnO NRs-AC) was successfully synthesized and the effects of carbon and zinc oxide were investigated for the photo-degradation of MG. Nanocomposite was characterized by X-ray diffraction (XRD) and field emission scanning electron microscopy (FE-SEM). Also to achieve valuable results regarding the efficiency of the photo-catalytic process, the Box-Behnken Design (BBD) was used instead of the conventional "one-factor-at-a-time" method. Using BBD, the interactions between the factors involved in the degradation efficiency, i.e. initial dye concentration, reaction time, and photocatalyst dosage, were evaluated.

Table.1 Characteristics of malachite green

Structure	Formula	Molar mass (g/mol)	λ_{\max} (nm)
	C ₂₃ H ₂₅ N ₃	364.911	618

2. Experimental procedure

2. 1. Materials and instrument

All the analytical grade reagents used including malachite green (MG), activated carbon (AC), Zn(CH₃COO)₂ · 2H₂O, hexamethylenetetramine, NaOH, and ethanol were obtained from Merck (Darmstadt, Germany). The test solutions were prepared daily by diluting the corresponding stock solutions to the desired concentrations. The wavelength of maximum absorbance is the wavelength along that the absorption spectrum where a substance has its strongest photon absorption. This value was obtained for malachite green at λ_{\max} =618 nm, because the maximum absorption for malachite green occurs in this area of wavelength. So, the malachite green concentration was determined at 618 nm [27]. As a result, the MG concentration was determined at 618 nm using a Shimadzu UV-visible1650 PC spectrophotometer. A BEL PHS-3BW pH-meter with a combined glass-Ag/AgCl electrode was used for adjustment of the solution pH. The X-ray diffraction

(XRD) patterns were obtained using an automated Philips X'Pert X-ray diffractometer with Cu K α radiation (40 kV and 30 mA) for 2 θ values over 10–80°. The shape and surface morphology of the nanoparticles were investigated using a field emission scanning electron microscope (FE-SEM, Hitachi S4160) under an acceleration voltage of 15 kV.

2-2. Synthesis of ZnO NRs-AC

ZnO NRs-AC was synthesized by the co-precipitation method. For this synthesis, 10 mL of a hexamethylenetetramine solution (0.5 M) was added to 10 mL of a Zn (CH₃COO)₂ solution (1 M). The solution pH was adjusted to 8.0. Then 1.0 g of AC was added to the mixture. The reaction mixture was heated to 70° C. The mixture was retained at 70° C for 12 h. ZnO NRs-AC was finally separated from the reaction mixture and washed with distilled water and ethanol to remove the impurities [20].

2-3 photodegradation process

The photo-catalytic activity of the catalyst was evaluated by degrading MG in an aqueous medium under UV irradiation. A 400 W mercury lamp was used for the UV irradiation. The temperature of the reactor was maintained at the ambient temperature using a cooling fan. The distance between the surface of the dye solution and the light source was about 40 cm. Before irradiation, the pH value for the dye solution was checked in 6.4, and a certain amount of the photo-catalyst (ZnO NRs-AC) was added to the dye solution. The solution was stirred in the dark for 20 min to reach an adsorption-desorption equilibrium. The dye solution was placed under a UV irradiation. At fixed time intervals, the certain volume of dye solution was withdrawn and centrifuged to remove the catalyst particles for analysis. The concentration of the dye solution was analyzed using UV-visible spectroscopy at its maximum absorption wavelength (618 nm). The degradation efficiency of the dye (%) was calculated according to the following equation: (%)degradation efficiency= (A₀-A_t)/A₀ ×100 (1) where A₀ and A_t are the initial and remaining dye adsorption at a given time t, respectively.

2-4. Experimental design

The response surface methodology (RSM) based on the Box-Behnken design (BBD) was used to optimize the MG degradation by the photo-catalytic process. The Design-Expert software (Design Expert 7.0.0) was used for the analysis of the experimental results obtained. The three factors initial dye concentration (mgL⁻¹) (X₁), amount of ZnO NRs-AC (mg) (X₂), and reaction time (min) (X₃) were studied for the photo-catalytic degradation process. The degradation efficiency of MG was chosen as the response parameter. Table 2 shows the values for the operational parameters involved in the experimental design. The mathematical relationship between the response and the operational parameters were described through Eq. (2):

$$Y = b_0 + \sum_{i=1}^n b_i x_i + (\sum_{i=1}^n b_{ii} x_i)^2 + \sum_{i=1}^{n-1} \sum_{j=i+1}^n b_{ij} x_i x_j \quad (2)$$

where Y is the predicated response; and b₀, b_i, b_{ij}, and b_{ii} are the constant linear, interaction, and quadratic coefficients, respectively. Also x_i and x_j are the coded values for the experimental parameters. For statistical calculations, the variables X_i were coded as xi according to the following relationship:

$$x_i = (X_i - X_0) / \delta X \quad (3)$$

where X₀ is the value for X_i at the center point, and δX presents the step change [21, 22].

Table. 2 Ranges of operational parameters for experimental design through BBD

Parameters	Ranges		
	-1	0	+1
Initial dye concentration (mgL ⁻¹)	30	50	70
Amount of ZnO-AC (mg)	8	14	20
Reaction time (min)	20	40	60

3. Results and discussion

3-1. Catalyst characterization

ZnO NRs-AC was characterized by X-ray diffraction (XRD) and field emission scanning electron microscopy (FE-SEM). X-ray diffraction was used to investigate the changes of phase structure and crystallite size of ZnO photocatalysts. The XRD patterns for ZnO NRs-AC structure were shown in Fig. 1. All diffraction peaks in line broadening of (100),

(002), (101), (102), (110), (103), (112) and (201) could matched well with the hexagonal wurtzite structure of ZnO that was agreed with the values in the standard card (JCPDS 36-1451) [25]. Also, It seems that the broad peak in $2\theta = 10-30$ is related to the amorphous phase of AC [28].

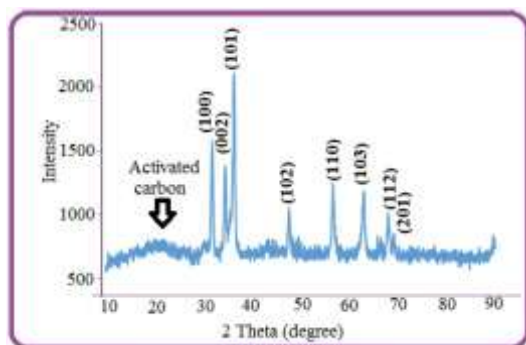


Fig. 1. XRD patterns for ZnO NRs-AC.

Fig. 2 shows the FE-SEM images for the AC and the ZnO NRs-AC. By comparing the morphologies for AC (Fig. 2a,) and ZnO NRs-AC (Fig. 2b), it is clear that surface morphology of the AC is homogeneous and relatively smooth (Fig. 2a), while the SEM images of the ZnO NRs-AC show that ZnO nanorods are well dispersed on the activated carbon. Fig 2b clearly shows the hexagonal structure of ZnO and growth direction along the wurtzite c axis. According to Fig. 2c average diameters of nanorods were between 80-200 nm.

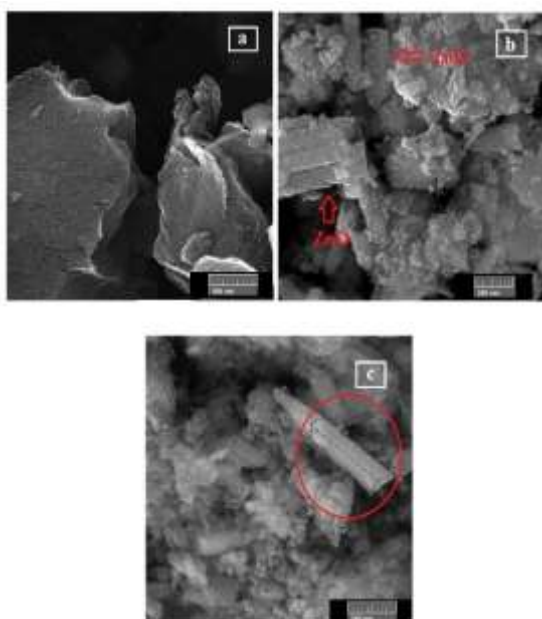


Fig. 2. (a) and (b,c) images are FE-SEMs for AC and ZnO NRs-AC, respectively.

3-2. Photo-catalytic activity

To evaluate the effect of ZnO NRs-AC on the degradation efficiency, experiments were carried out using ZnO NRs-AC/UV and UV alone (photolysis). The results obtained are shown in Fig. 3 (a,b). The photolysis process carried out using a UV lamp alone showed a degradation efficiency of 5% after 100 min, while the degradation efficiency was 100% in the presence of ZnO NRs-AC with exposure to UV light after 100 min.

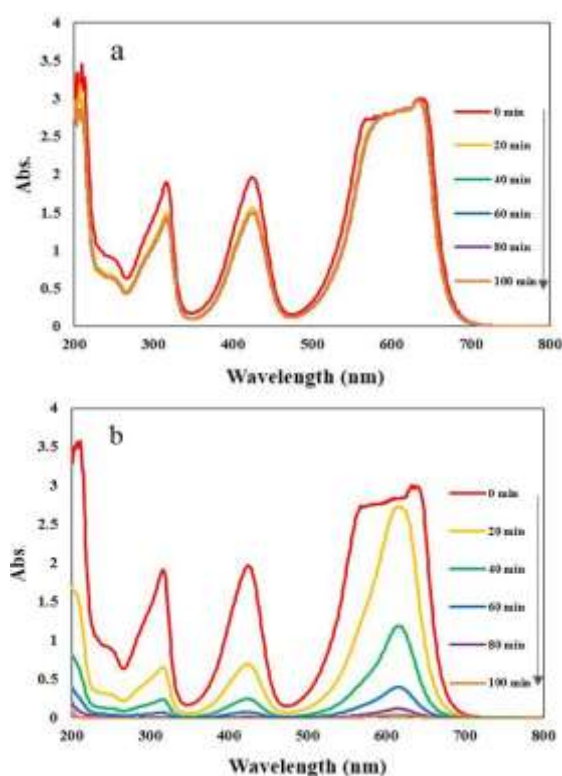


Fig. 3. UV-visible absorption spectra for MG degradation (a) in the absence of catalyst, and (b) in the presence of catalyst.

Experimental conditions: [MG], 70 mgL⁻¹; [catalyst], 20 mg; pH, natural.

3-2-1. Degradation mechanism

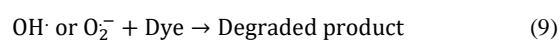
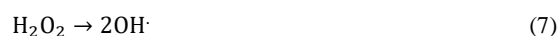
Due to a rapid recombination, their electrons return again from the excited state to the initial state. As a result, the degradation process by the dye alone (photolysis) and the AC alone (absence of UV radiation) could not be successful. AC, as a bed for ZnO, plays an important role in the degradation process. When ZnO is placed on the surface of AC, the degradation efficiency is expected to increase because AC increases the surface area available for adsorbing

the dye molecules. When the photocatalyst is exposed to the UV light, ZnO can absorb the light and the electrons are transferred from VB to CB and generate electron-hole pairs. The CB electrons can react with the oxygen molecules adsorbed on the catalyst surface to form oxygen radicals (O_2^-). Then these radicals react with H_2O molecules to form $\cdot OH$ radicals. Also the holes in VB can react with H_2O molecules to form $\cdot OH$ radicals. These radicals, as strong oxidizing species, and O_2^- are responsible for the degradation of MG. According to this mechanism, the excited electrons in AC are transferred to CB of ZnO. As a result, with more electrons transferred to the dye solution, the degradation efficiency increases [23, 24].

Table. 4 ANOVA test results for degradation of malachite green by photocatalytic process.

Source	Sum of squares	df	Mean square	F-Value	P-Value
Model	15729.7	9	1747.75	34.20	<0.0001
X ₁	8099.4	1	8099.4	158.51	<0.0001
X ₂	5390.8	1	5390.8	105.50	<0.0001
X ₃	1604.6	1	1604.6	31.40	0.0008
X ₁ X ₂	237.6	1	237.6	4.6	0.0680
X ₁ X ₃	138.0	1	138.0	2.7	0.1442
X ₂ X ₃	63.2	1	63.2	1.2	0.3028
X ₁ ²	14.20	1	14.20	0.28	0.6143
X ₂ ²	89.2	1	89.2	1.7	0.2279
X ₃ ²	89.3	1	89.3	1.7	0.2277
Residual	357.6	7	51.1		
Lack-of-fit	257.8	3	85.9	3.4	0.1318
Pure error	99.8	4	24.9		
Total	16087.3	16			

$R^2=0.9778$, adjusted $R^2=0.9492$, adequate precision= 21.077, coefficient of variation (CV)= 12.54.



3-2-2 Model results for degradation

According to RSM based on BBD, there is a relationship between the dependent parameter (degradation efficiency) and the independent parameters involved in the photo-catalytic process (Eq.10):

$$Y=60.47-31.82 x_1+25.96x_2+14.16x_3+1.84x_1^2-4.6x_2^2-4.61x_3^2+7.71x_1 x_2-3.98x_2 x_3+5.88x_1 x_3 \quad (10)$$

The experimental results for the degradation efficiency are presented in Table 3. To determine the significant parameters involved and the proposed model for the dye degradation, the analysis of variance (ANOVA) test was used (Table 4). The model F-value of 34.20 implies that the model is significant. The "prob > F" values less than 0.05 indicate that the model terms are significant at a confidence level of 95%. Values greater than 0.10 indicate that the model terms are not significant. In this case, X₁, X₂, and X₃ are significant model terms. X₁X₂ is significant at a confidence level of 90% and less significant than X₁, X₂, and X₃. The "lack-of-fit P-value" of 0.1318 implies that the lack-of-fit is not significant. A non-significant lack-of-fit represents the fitness of the model.

There is no significant difference between the values for R² (0.9778) and adjusted R² (0.9492), and this demonstrates the significance of the model. "Adeq Precision" measures the signal-to-noise ratio. A ratio greater than 4 is desirable. Thus a ratio of 21.077 in the present work implies the suitability of the model. The coefficient of variation value of 12.54% indicates a good reliability of the model.

Fig. 4a represents a plot of the predicted versus the experimental degradation efficiency. This figure shows a good agreement between the predicted and experimental degradation efficiency ($R^2=0.9778$) and represents the adequacy and significance of the model. Fig.4b indicates the normal plots of the predicted vs. the observed response for the degradation efficiency. As it is evident in this figure, the data points obtained consistently appear on a straight trend line, demonstrating that there is no obvious dispersal. Dispersal of residuals is shown in Fig. 4c.

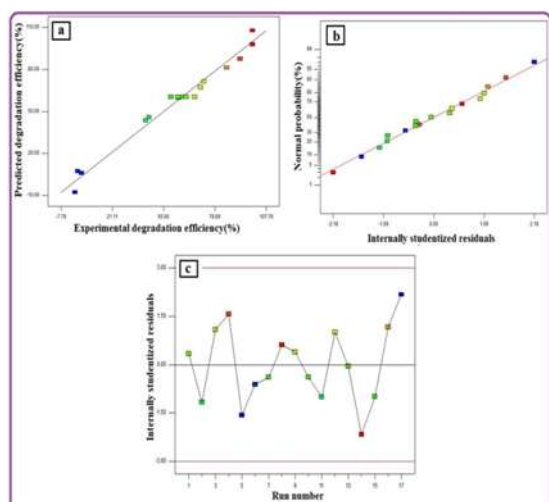


Fig. 4. Plot of predicted versus experimental degradation efficiency (%) (a); plot of normal probability versus residuals (b); plot of residuals versus run number (c).

3-2-3. Interactive effects of operational parameters on degradation efficiency

Response surface and contour plots were used to investigate the interactive effects of the factors involved on the degradation efficiency. The interaction effects of the photocatalyst dosage and initial dye concentration on the efficiency of the MG photo-catalytic degradation, illustrated in Figs 5a to 5c show that the degradation efficiency increases with increase in the ZnO NRs-AC dosage from 8 to 20 mg and decrease in the initial dye concentration from 70 to 30 mg.L⁻¹. The effect of the initial dye concentration was more significant at higher ZnO NRs-AC dosages. The effect of ZnO NRs-AC dosage was more significant at lower initial dye concentrations, and this means that a higher dye concentration has a more coating effect on the catalyst surface. Therefore, the transmission of light to the ZnO NRs-AC surface and the absorption of light by the catalyst can be reduced. As a result, fewer electrons can be excited from the VB to the CB of ZnO-AC. Finally, the generated hydroxyl radicals can decrease the degradation efficiency. Also an increase in the degradation efficiency with an increase in the amount of catalyst can be justified by the fact that the active sites on the catalyst surface increase; more dye molecules are placed on the

Table. 3 Experimental results of applied model for photo-catalytic malachite green degradation over ZnO NRs-AC

Run	Initial dye conc. (mg.L ⁻¹)	ZnO-AC dosage (mg)	Reaction time (min)	Degradation efficiency (%)
1	50	14	40	62.69
2	70	14	60	41.74
3	50	14	40	67.43
4	50	20	60	93
5	50	8	20	1.58
6	70	14	20	3.66
7	70	20	40	58.15
8	30	14	60	100
9	30	8	40	72.68
10	50	14	40	58.01
11	50	8	60	39.85
12	50	20	20	70.63
13	50	14	40	60.12
14	30	20	40	100
15	50	14	40	54.12
16	30	14	20	85.42
17	70	8	40	0

catalyst holes and absorbed by the catalyst. Accordingly, the adsorbed dye molecules degrade quickly [23, 29].

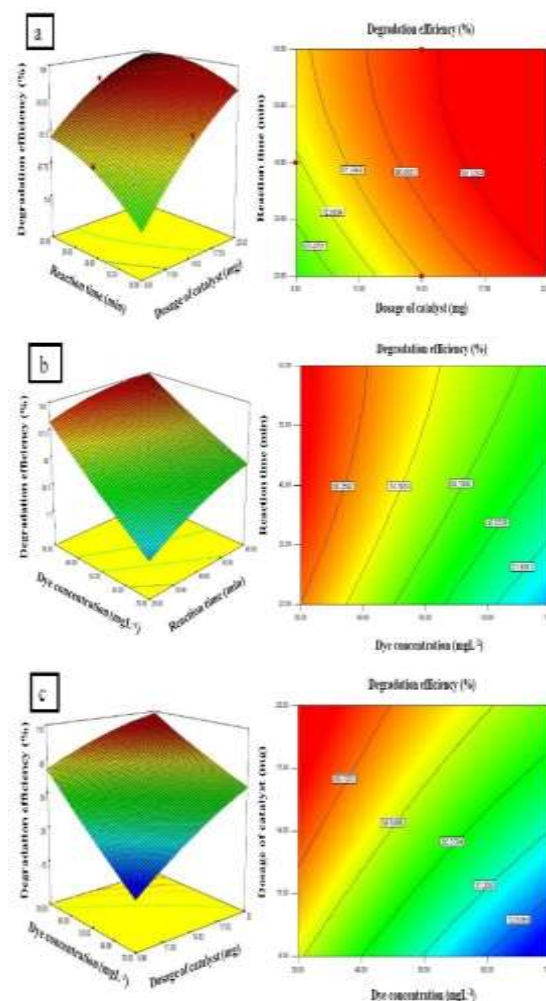


Fig. 5. Response surface plot and corresponding counter-plot of malachite green degradation as a function of initial dye concentration (mg.L⁻¹) and ZnO NRs-AC dosage. pH: 6.4, reaction time: 46 min.

3-2-4. Degradation optimization

To achieve the maximum degradation efficiency, the operational parameters involved were optimized in the studied ranges. As a result, the optimum conditions were obtained to be an initial dye concentration of 30 mg.L⁻¹, a reaction time of 46 min, and a ZnO NRs-AC dosage of 16 mg. The maximum degradation efficiency of the model was predicted to be 100% under the optimal conditions (Table 5). To validate the optimal parameters, three experiments were carried out to confirm the degradation efficiency. These experiments showed a degradation efficiency of 100% under the optimal conditions. This indicates the suitability and accuracy of the model.

Table 5 Optimum values for parameters for a degradation efficiency of 100%.

Parameter	Optimum value
Initial dye concentration (mg.L ⁻¹)	30
ZnO-AC dosage (mg)	16
Reaction time (min)	46

3-3. Interference study

There are various pollutants in urban wastewaters, in which the existence of some foreign ions can cause a disturbance in the photo-catalytic degradation processes. The effects of these ions on the photo-catalytic processes are important in determining the stability of photo-catalyst in the photo-catalytic water treatment process. In this work, we investigated the effects of the Ca²⁺, Na⁺, Mg²⁺, Cl⁻, HCO₃⁻, HPO₄²⁻, NO₃⁻, and SO₄²⁻ ions on the dye degradation process. For this purpose, different concentrations of these ions were examined under the optimal conditions. According to the amounts of mean (\bar{X}) and standard deviation (S) obtained from three replicate degradation efficiency measurements under the optimum conditions and according to ($\bar{X} \pm 3S$), the maximum concentrations of these ions for existence of interference were obtained (Fig.6). If the degradation efficiency of the dye solutions containing various amounts of ions exists in the range of ($\bar{X} \pm 3S$), there will be no interference effect on the photo-catalytic

activity of ZnO NRs-AC [25]. Fig.6 shows that the Cl⁻ and Mg²⁺ ions had more interference effects on the dye degradation; they had interference effects at concentrations greater than 100 and 300 mg.L⁻¹, respectively. The other ions did not have any considerable interference effect on the photo-catalytic activity of ZnO NRs-AC even at the high concentration of 1000 mg.L⁻¹.

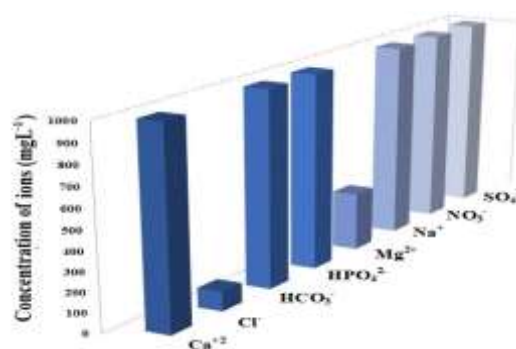


Fig. 6. Interference study results for degradation of MG solution.

3-4 Kinetic study

Studying the reaction kinetics is important for appointing the parameters affecting the reaction rate. The aim of this study was to find a suitable kinetic model for the photo-catalytic degradation reaction. For this purpose, The rate constant (k) and the correlation coefficient (R^2) of dye degradation by ZnO NRs-AC at different MG concentrations were studied by zero- (Eq. (11)), first- (Eq. (12)), and second-order (Eq. (13)) kinetics (Table 6).

$$[C] = -k_0 t + [C]_0 \quad (11)$$

$$\ln [C]_0 / [C] = k_1 t \quad (12)$$

$$1/[C] - 1/[C]_0 = k_2 t \quad (13)$$

where C is the MG concentration in an aqueous solution at time t (mg.L⁻¹); C_0 is the initial MG concentration (mg.L⁻¹); and k_0 (mg.L⁻¹min⁻¹), k_1 (min⁻¹), and k_2 (L.mg⁻¹min⁻¹) are the zero-, first-, and second-order rate constants, respectively. The results obtained showed that the kinetics of the degradation using ZnO NRs-AC followed a first-order kinetic model. According to many articles, the degradation kinetics of most dyes by the heterogeneous photo-catalytic method fitted to the Langmuir-Hinshelwood (L-H) kinetic model (Eq. (14)) [28, 30].

$$r_0 = -(dC_0)/dt = (kKC_0)/(1+kC_0) \quad (14)$$

where k is the adsorption coefficient of the reaction, K is the rate constant of the reaction, and r_0 is the initial rate of degradation. Integrating Eq. (14) gives:

$$-dC_0(1+kC_0) = kKC_0 dt \quad (15)$$

$$\int_{C_0}^C -\frac{1+kC_0}{kKC_0} dC_0 = \int_0^t dt \quad (16)$$

$$\frac{-1}{kK} \int_{C_0}^C \frac{dC_0}{C_0} - \frac{1}{K} \int_{C_0}^C dC_0 = \int_0^t dt \quad (17)$$

$$t = \frac{1}{kK} \ln\left(\frac{C_0}{C}\right) + \frac{1}{K}(C_0 - C) \quad (18)$$

When the concentration of the dye is low, by ignoring the term $(C_0 - C)$, Eq. (18) changes to a pseudo-first-order kinetic model (Eq. (20)) [31].

$$t = \frac{1}{kK} \ln\left(\frac{C_0}{C}\right) \quad (19)$$

$$\ln\left(\frac{C_0}{C}\right) \approx kKt \xrightarrow{kK=k_{app}} \ln\left(\frac{C_0}{C}\right) \approx k_{app}t \quad (20)$$

Table 6 Kinetic parameters for MG degradation during 120 min

	Dye concentration (mgL ⁻¹)			R ²
	30	50	70	
k_0	0.014	0.024	0.024	0.836
R ²	0.62	0.91	0.98	
k_1	0.101	0.043	0.017	0.986
R ²	0.992	0.983	0.983	
k_2	145.17	0.755	0.025	0.815
R ²	0.812	0.741	0.893	

By plotting $\ln(C_0/C)$ versus t , a straight line was obtained (Fig. 7). The slope of this line represents the apparent rate constant (k_{app}). Fig. 7 shows that the photo-catalytic degradation fit to the Langmuir–Hinshelwood kinetic model. As a result, the kinetic of degradation followed a pseudo-first-order kinetic model. The amount of k_{app} was obtained to be 0.101, 0.043, and 0.017 for the dye concentrations of 30, 50, and 70 mg.L⁻¹, respectively. According to Fig. 7 and the amount of k_{app} , the degradation rate decreased with increase in the dye concentration.

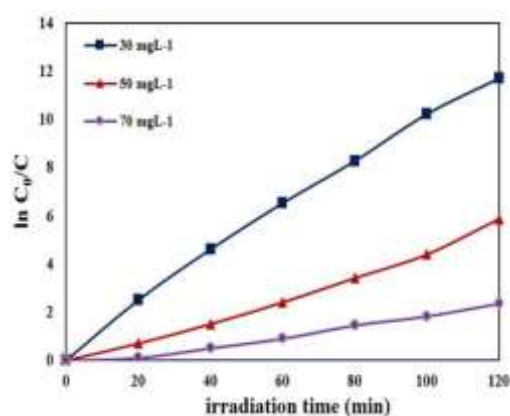


Fig. 7. Plot of $\ln(C_0/C)$ versus irradiation time for different initial concentrations of MG.

4. Reusability of photocatalyst study

To investigate the usefulness of the synthetic photocatalys, ZnO NRs-AC was tested in the optimum conditions for several times. The results presented in Table 7 show the excellent stability of the photocatalyst after 5 times usage of it.

Table 7. Results obtained for repeated use of ZnO NRs-AC after cyclic regeneration.

Recovery (%)	Repetitions					
	1	2	3	4	5	6
MG	100	100	97	94	90	82

5. Comparison

In order to show the capabilities of the proposed method with other methods, the comparison between the proposed work with previous works was done. According to Table 8, The proposed photocatalyst relative to presented photocatalysts have the following abilities:

- 1- High degradation percentage was observed in high concentration dye solution compared to other methods
- 2- The photodegradation of dye is fast so that the whole process is performed in 46 min.
- 3- With the least amount of photocatalyst, compared with the other photocatalyst, a maximum recovery was obtained.

Table 8. Results obtained for repeated use of ZnO NRs-AC after cyclic regeneration.

Photo catalyst	Dye	Amount (mg)	Concentration (ppm)	Time (min)	Ref
ZnO nano-baskets	RG ¹	100	10	90	[32]
ZnO	MB ²	20	20	80	[33]
ZnO	MB	10	5	150	[34]
ZnO nanoplates	MB	200	3	240	[35]
ZnO nano-corncoobs	MO ³	150	20	180	[36]
ZnO-AC	MG ³	16	30	46	This work

¹ Rodamin 6G² Methylene blue³ Methyl Orange

6. Conclusion

ZnO nanostructure –AC (ZnO NRs-AC) with well-defined rods morphology was prepared and used as a new photo-catalyst for the degradation of MG under UV irradiation. The effective parameters were efficiently optimized through the Box-Behnken design. According to RSM based on BBD, a 100% degradation efficiency was gained under the optimal conditions (initial dye concentration, 30 mg.L⁻¹; ZnO NRs-AC, 16 mg; and reaction time, 46 min). The results of the kinetic study of the photo-catalytic degradation reaction showed that the kinetic of the degradation using ZnO NRs-AC followed a pseudo-first-order kinetic model. Finally, ZnO NRs-AC was shown a high photo-catalytic activity for the degradation of MG with a high concentration in less than two hours.

Acknowledgment

The authors wish to thank the Department of Chemistry in the Semnan university for the support of this work.

References

- [1] G. Crini, *Bioresource Technology*, **97** (2006) 1061.
- [2] A.R. Fischer, P. Werner, K.U. Goss, *Chemosphere*, **82** (2011) 210.
- [3] M.S. Rahbar, E. Alipour, R.E. Sedighi, *International Journal of Environmental Science & Technology*, **3** (2006) 79.
- [4] D. Méndez-Paz, F. Omil, J.M. Lema, *Anaerobic, Enzyme and Microbial Technology*, **36** (2005) 264.
- [5] M. Mousavi-Kamazani, R. Rahmatolahzadeh, S. A. Shobeiri, *Journal of Materials Science: Materials in Electronics*, **28** (2017) 17961.
- [6] N. Azbar, T. Yonar, K. Kestioglu, *Chemosphere*, **55** (2004) 35.
- [7] S. A. Shobeiri, M. Mousavi-Kamazani, F. Beshkar, *Journal of Materials Science: Materials in Electronics*, **28** (2017) 8108.
- [8] M. Mousavi-Kamazani, Z. Zarghami, R. Rahmatolahzadeh, M. Ramezani, *Advanced Powder Technology*, **28** (2017) 2078.
- [9] A. M. Latifi, M. Mirzaei, M. Mousavi-Kamazani, Z. Zarghami, *Journal of Materials Science: Materials in Electronics*, **29** (2018) 10234.
- [10] C. Galindo, P. Jacques, A. Kalt, *Chemosphere*, **45** (2001) 997.
- [11] M. Goudarzi, M. Mosavi-Kamazani, M. Salavati-Niasari, *Journal of Materials Science: Materials in Electronics* **28** (2017), 8423.
- [12] S.K. Kansal, N. Kaur, S. Singh, *Nanoscale Research Letters*, **4** (2009) 709.
- [13] Z. Li, Y. Fang, S. Xu, *Materials Letters*, **93** (2013) 345.

- [14] R. Khan, M.S. Hassan, H.-S. Cho, A.Y. Polyakov, M.-S. Khil, I.-H. Lee, *Materials Letters*, **133** (2014) 224.
- [15] D. Li, K. Dai, J. Lv, L. Lu, C. Liang, G. Zhu, *Materials Letters*, **150** (2015) 48.
- [16] H. Hu, C. Deng, J. Xu, Q. Zheng, G. Chen, X. Ge, *Materials Letters*, **161** (2015) 17.
- [17] J. Lin, S. Pang, Q. Wang, *Materials Letters*, **98** (2013) 12.
- [18] J. Chaisorn, K. Wetchakun, S. Phanichphant, N. Wetchakun, *Materials Letters*, **160** (2015) 75.
- [19] W.G. Xu, S.F. Liu, S.X. Lu, S.Y. Kang, Y. Zhou, H.F. Zhang, *Journal of Colloid and Interface Science*, **351** (2010) 210.
- [20] M. Ghaedi, M.N. Biyareh, S.N. Kokhdan, S. Shamsaldini, R. Sahraei, A. Daneshfar, S. Shahriyar, *Materials Science and Engineering: C*, **32** (2012) 725.
- [21] R. Darvishi Cheshmeh Soltani, A. Rezaee, A.R. Khataee, H. Godini, *The Canadian Journal of Chemical Engineering*, **92** (2014) 13.
- [22] A.R. Khataee, M. Zarei, S.K. Asl, *Journal of Electroanalytical Chemistry*, **648** (2010) 143.
- [23] P. Raizada, P. Singh, A. Kumar, G. Sharma, B. Pare, S.B. Jonnalagadda, P. Thakur, *Applied Catalysis A: General*, **486** (2014) 159.
- [24] L. Saikia, D. Bhuyan, M. Saikia, B. Malakar, D.K. Dutta, P. Sengupta, *Applied Catalysis A: General*, **490** (2015) 42.
- [25] M. Arab Chamjangali, G. Bagherian, B. Bahramian, B. Fahimi Rad, *International Journal of Environmental Science and Technology*, **12** (2015) 151.
- [26] C.-C. Mao, H.-S. Weng, *Chemical Engineering Journal*, **155** (2009) 744.
- [27] F. Zhang, Z. Wei, W. Zhang, H. Cui, *Spectrochimica Acta Part A: Molecular and Biomolecular Spectroscopy*, **182** (2017) 116.
- [28] F. Lu, C. Huang, L. You, J. Wang, Q. Zhang, *RSC Advance*, **7** (2017) 23255-23264.
- [29] C.G. da Silva, J.L.s. Faria, *Journal of Photochemistry and Photobiology A: Chemistry*, **155** (2003) 133.
- [30] K.V. Kumar, K. Porkodi, F. Rocha, *Catalysis Communications*, **9** (2008) 82.
- [31] V. Mirkhani, S. Tangestaninejad, M. Moghadam, M.H. Habibi, A.R. Vartooni, *Journal of the Iranian Chemical Society*, **6** (2009) 800.
- [32] S. Ameen, M.S. Akhtar, H.S. Shin, *Materials Letters*, **183** (2016) 329.
- [33] T. Cun, C. Dong, Q. Huang, *Applied Surface Science*, **384** (2016) 73.
- [34] A.N. El-Shazly, M.M. Rashad, E.A. Abdel-Aal, I.A. Ibrahim, M.F. El-Shahat, A.E. Shalan, *Journal of Environmental Chemical Engineering*, **4** (2016) 3177.
- [35] A. Phuruangrat, S. Thongtem, T. Thongtem, *Materials & Design*, **107** (2016) 250.
- [36] C. Gomez-Solís, J.C. Ballesteros, L.M. Torres-Martínez, I. Juárez-Ramírez, L.A. Díaz Torres, M. Elvira Zarazua-Morin, S.W. Lee, *Journal of Photochemistry and Photobiology A: Chemistry*, **298** (2015) 49.